Food Biophysics (2018) 13:343–352
https://doi.org/10.1007/s11483-018-9540-9

ORIGINAL ARTICLE

Encapsulation of Bixin with High Amylose Starch as Affected by Temperature and Whey Protein

Ezequiel José Pérez-Monterroza[1] · Ana María Chaux-Gutiérrez[1] · Célia Maria Landi Franco[1] · Vânia Regina Nicoletti[1]

Received: 18 February 2018 / Accepted: 20 June 2018 / Published online: 26 June 2018

Abstract

Microencapsulation of bixin using high-amylose corn starch was carried out by the acidification method. Bixin powders were characterized by differential scanning calorimetry (DSC), X-ray diffractometry (XRD), FT-IR spectrometry, color parameters, encapsulation efficiency, bixin release profile. In addition, the effect of whey protein (WP) on the microencapsulation process was investigated. The results obtained from DSC, X-ray diffraction and FT-IR spectrometry indicated that only in the samples prepared at 90 °C (B0WP90°C, B10WP90°C, and B20WP90°C) there was formation of crystalline structures, with melting temperatures at 117.2°, 105° and 104 °C, respectively. The possible interactions between bixin, WP and amylose starch are also discussed.

Keywords Annatto · Microencapsulation · Melting enthalpy · Release characteristics

Introduction

The seeds of the tropical plant *Bixa Orellana*, which grows in Central and South America, are the source of Annatto, a natural dye that has been used as a yellow to orange food colorant and has widespread usage in dairy and fat-based products such as butter, cheese, margarine, meat and snacks. Annatto extracts are prepared by solvent extraction of the seeds and contains bixin as the major pigment. Bixin is an oil-soluble apocarotenoid that has the characteristic isoprenoid structure of the carotenoid pigments, but with a much shorter chain length of 26 carbons, presenting a carboxylic acid group at one end, and a methyl ester at the opposite end [1, 2]. Bixin has a good antioxidant capacity, it is able to sequester free radicals due to high flavonoids, tocopherol, and carotenoid contents. It has potential to be used as a chemo-preventive in current cancer therapies, decreasing the adverse effects of antitumoral agents [3–5]. Also, bixin has δ-tocotrienols, which are used in cardiovascular diseases and cancer [6]. Nevertheless, bixin can be oxidized by light and can be affected by elevated temperatures, but their major cause of instability is the contact with atmospheric oxygen [7]. For this reason, microencapsulation may be a feasible alternative to improve the stability of these bioactive compounds. The microencapsulation of bixin can be carried out using chitosan, gum Arabic, or maltodextrin by spray drying [8, 9]. Also, as it was reported by De Sousa Lobato et al. [10], bixin can be microencapsulated by interfacial deposition on preformed poly(ε-caprolactone). Encapsulation by complexation with amylose is an alternative that could be applied to protecting bixin against oxidation, as well as for developing controlled delivery systems. Bixin can form inclusion complexes with α-cyclodextrin and β-cyclodextrin [11, 12] and, due to the similarity between the hydrophobic helical cavity of amylose with that of cyclodextrin, it is reasonable to consider the possibility of producing amylose-bixin complexes. It is known that the amylose present in starch granules can form inclusion complexes with hydrophobic molecules such as alcohols, flavors, aromas, fatty acids and nutraceutical compounds [13–17]. These are called V-type inclusion complexes, which are formed when a hydrophobic molecule is entrapped inside of an amylose helix cavity. Diffraction patterns of amylose

Electronic supplementary material The online version of this article (https://doi.org/10.1007/s11483-018-9540-9) contains supplementary material, which is available to authorized users.

✉ Ezequiel José Pérez-Monterroza
eperez494@gmail.com; ejperezm@unalmed.edu.co

[1] Department of Food Engineering and Technology, São Paulo State University (Unesp), Institute of Biosciences, Humanities and Exact Sciences (Ibilce), Rua Cristovão Colombo 2265, São José do Rio Preto, São Paulo Zip Code 15054-000, Brazil

complexes suggest that V-type complexes might be formed by six (V_6), seven (V_7) or eight (V_8) glycosyl residues per helical turn, and their diameters depend on the structure and size of the guest molecule [18, 19].

On the other hand, the encapsulation process based on starch can be affected by the presence of proteins, which could affect the release characteristics of the system. In fact, whey protein can compete for a guest molecule by forming a three-in-one complex, affecting the amount of complex formed [20]. Proteins can interact with themselves or with polysaccharides after of the denaturation process, leading to conformational changes in the blends [21]. Additionally, the denaturation process increases the affinity of the protein by bixin [22]. For the above, it is reasonable to consider the possibility of producing an encapsulation system composed of whey protein, bixin, and starch. In this matrix, the protein is the trigger of the release system, due to its ability to act as an access barrier for digesting enzymes and against diffusion of the encapsulated bixin, which allows preparation of controlled delivery systems. Hence, this work presents the results of bixin encapsulation with high-amylose corn starch, including the characterization of the produced bixin powder, as well as the effect of whey protein on the microencapsulation.

Material and Methods

High-amylose (72% of amylose, according to manufacturer) corn starch (Hylon VII) was obtained from Ingredion Brasil Ing. Ind. Ltda (Mogi Guaçu, SP, Brazil). Bixin was obtained from BKG (Adicon, Brazil). Whey protein concentrate (WP) was obtained from Alibra ingredients Ltda (SP, Brazil). Sodium hydroxide (NaOH) was supplied by Synth (Diadema, Brazil), hydrochloric acid was provided by Quimis (Diadema, Brazil), and pancreatin was provided by Sigma-Aldrich (St. Louis, MO). Starch suspensions were prepared using deionized water. All chemicals were of analytical grade.

Microencapsulation

Ninety grams of high-amylose corn starch (Hylon VII) in 2350 g of water were gelatinized at 130 °C for 45 min. One hundred and fifty grams of the gelatinized starch suspension (GS) was mixed with bixin (0.3 g) in 0.01 M KOH solution (50 g) at temperatures of 60, 70, and 90 °C for 60 min, followed by precipitation at pH 4.5 using 0.01 M HCl. The precipitate was separated by centrifugation at 9000×g for 10 min, was cooled at −18 °C for 12 h and lyophilized. When the use of protein (WP) was necessary, it was added to the gelatinized starch suspension according to Table 1. The samples were coded with the letter B followed by whey protein ratio and temperature of treatment. A control sample (GS-B), consisting of GS (150 g) and bixin (0.3 g) in 0.01 M KOH solution (50 g), was prepared at 45 °C for 1 min. Also, a control sample (GS-WP), consisting of GS (150 g) and WP (1.24 g), was prepared at 60, 70 and 90 °C for 60 min.

Differential Scanning Calorimetry (DSC)

The thermal characterization of the samples was carried out by analyzing the thermograms obtained in a PerkinElmer DSC 8000 (PerkinElmer Corp, Shelton, CT, USA). The equipment was calibrated with indium before analysis. Nitrogen was used as a purge gas for the system. For the analysis, 4–5 mg of the samples were weighed in aluminum pans. An empty aluminum pan was used as the reference. The samples were heated at 10 °C/min from 80 to 140 °C, then subsequently cooled at 10 °C/min from 140 to 80 °C. The results of the thermal analyses were processed using PerkinElmer Pyris software, version 10.0 (PerkinElmer Inc., Shelton, CT, USA).

X-Ray Diffraction (XRD)

X-ray diffraction was carried out with a diffractometer RINT 2000 wide angle Goniometer unit (Rigaku, Tokyo, Japan). The diffractometer was operated at a voltage of 45 kV and a current of 40 mA. The samples were scanned from 5° to 40° in 2θ, at a rate of $1°{\cdot}min^{-1}$ and a step size of 0.1°. The relative crystallinity was calculated based on the relationship between the peak area and total area of the X-ray diffractograms, according to Itthisoponkul et al. [13], by using Origin software (Microcal Inc., Northampton, USA). Diffractograms were smoothed and the baseline was corrected. The analyses were carried out in duplicate.

FT-IR Spectroscopy

Infrared spectra were recorded on a Spectrum One spectrophotometer (PerkinElmer Corp, Shelton, CT, USA) with an attenuated total reflectance accessory and a ZnSe crystal. Samples were analyzed directly after pressing them on the crystal (80 psi), and FT-IR scanning was conducted at ambient conditions. The resolution was set to 4 cm^{-1}, and the operating range was set to 400 to 4000 cm^{-1}. In all cases, 20 scans per sample were recorded. The data were processed using Origin Pro 8 Software (Microcal Inc., Northampton, USA). The analyses were carried out in duplicate.

Encapsulation Efficiency EE (%)

The surface and encapsulated bixin content in the samples was determined according to Lalush et al., [14] and Sutter, Buera, and Elizalde [23], with modifications. Surface bixin was determined by washing 0.010 g of the complex with 4 mL of acetone in a test tube and shaking the mixture in a vortex for 2 min. After sedimentation, the powder was separated and the

Table 1 Values of encapsulation efficiency

	Samples	WP (%)	WP (g)	Encapsulation efficiency EE (%)
Temperature treatment 60 °C	B0WP60°C	0	0	63.64
	B10WP60°C	10	0.6	82.46
	B20WP60°C	20	1.24	28.30
temperature treatment 70 °C	B0WP70°C	0	0	24.30
	B10WP70°C	10	0.6	57.05
	B20WP70°C	20	1.24	34.51
temperature treatment 90 °C	B0WP90°C	0	0	23.30
	B10WP90°C	10	0.6	82.91
	B20WP90°C	20	1.24	62.91
	GS-B	–	–	33.29

concentration of bixin in the acetone was measured spectrophotometrically at 457 nm. Encapsulated bixin in the remaining powder was determined by degradation of the complex with pancreatin. The powder was incubated in 4 mL of pancreatin solution at 37 °C for 36 h. Then, bixin was extracted with 7 mL of acetone, centrifuged, filtered and quantified spectrophotometrically at 457 nm. This wavelength was found to correspond to the maximum absorbance of the used bixin, in the spectrum range of 200 to 600 nm. For preparing the pancreatin solution, 0.18 g of pancreatin was dissolved in 20 mL of phosphate buffer 20 mM (pH 7.0) containing NaCl (0.04% *w*/w). This solution was centrifuged (9000×g, 10 min), and the supernatant was filtered and used for the test. Bixin content in the complex was calculated for each formulation as μg of bixin per g of total complex [24, 25]. To calculate Encapsulation efficiency Eq. 1 was used [26]. The analyses were carried out in duplicate.

$$\mathrm{EE}\ (\%) = \frac{\mathrm{Bi}}{(\mathrm{Bi} + \mathrm{Bo})} \times 100 \tag{1}$$

Bi Bixin content retained inside of matrix
Bo Bixin content retained on surface of matrix

Release Profile of Bixin in Simulated Intestinal Fluid

Determination of the release profile was carried out according to Lesmes et al., [27] with modification. The complexes (0.010 g) were dispersed in 15 mL of simulated intestine fluid (SIF), which was prepared by dissolving 0.18 g of pancreatin in a phosphate buffer solution (20 mM, pH 7.0) containing NaCl (0.04% *w*/w). This dispersion was centrifuged (9000×g, 10 min), and the supernatant was filtered and used to incubate the complexes at 37 °C. At intervals of time (30, 60, 90, 150, 210 and 270 min), aliquots of 1 mL of this dispersion were separated and immediately subjected to bixin extraction with 4 mL of acetone, which was centrifuged and measured spectrophotometrically at 457 nm. The volume taken was replaced with fresh SIF. The analyses were carried out in duplicate.

Color Analysis

The color of the samples was determined using a ColorFlex model 45/0 spectrophotometer (Hunterlab, USA) with the D65 illuminant and observer at 10°. The 4.10 version of Universal software was used to determine the absolute values of L*, a*, and b*. The system used for specification of color was CIELAB. Values of L* (lightness) range between zero (black) and one hundred (white), a* between -a* (green) and + a* (red), and b* between -b* (blue) and + b* (yellow). The chroma (C*), which expresses the degree of intensity or saturation of the color (Eq. 2), and the hue angle (°hue), which represents the tonality of the color (Eq. 3), were calculated. The analyses were carried out in triplicate.

$$C^* = \sqrt{(a^*)^2 + (b^*)^2} \tag{2}$$

$$^{\circ}hue = arctg\left(\frac{b^*}{a^*}\right) \tag{3}$$

Results and Discussion

Differential Scanning Calorimetry (DSC)

DSC analysis was performed on encapsulated bixin (Fig. 1a). Samples B0WP90°C, B10WP90°C, B20WP90°C, which were prepared at 90 °C, showed an endothermic peak at 117.2, 105, and 104 °C respectively, which were similar to V-type amylose complexes melting temperature. The melting

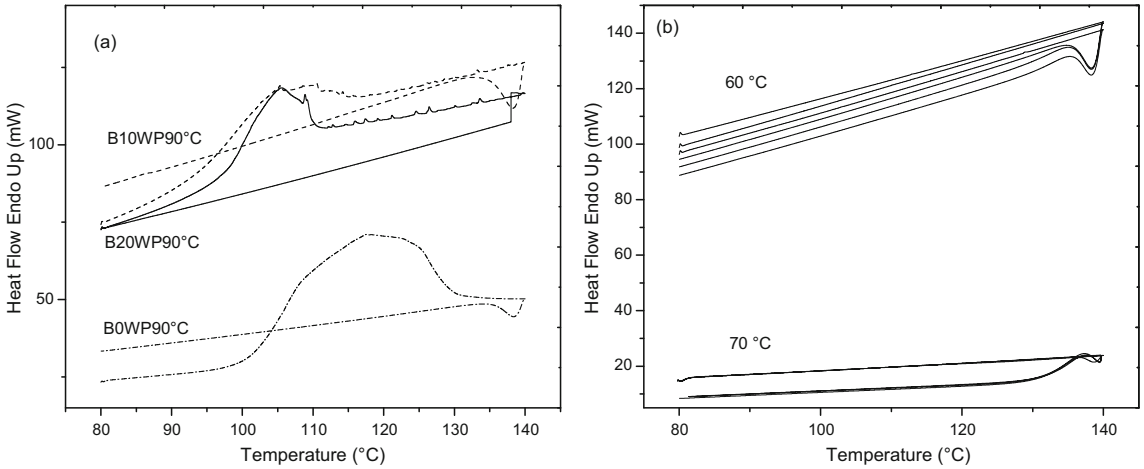

Fig. 1 Differential scanning calorimetry of bixin complexes prepared at 90 °C (**a**). Samples prepared at 60 and 70 °C (**b**)

was not thermally reversible since the endothermal transitions in the second scan were not observed. The crystalline structures do not return to its initial state after the cooling stage because the rate of heating and cooling used in DSC analysis are higher than those used during of preparation of samples. The necessary time to form these structures at 90 °C seems to be higher than that used in the heating and cooling stages, which makes difficult the recrystallization after them have melted during DSC analysis. This behavior was observed in other systems as these formed by b-carotene and starch dextrin, the cooling and heating used during DSC analysis migth not be a ideal kinetical process to regenerate crysline structures [28]. The melting temperatures of samples are similar to the type-II V-amylose complexes, which are characterized by forming partially-ordered structures, with different amorphous and crystalline regions. These complexes have melting temperatures above 100 °C and are excellent matrices with great resistance to heat [15, 29]. Although the formation of amylose bixin complex was not confirmed by X-ray diffration, the crystalline structure formed offer high thermal resistance, melting above 100 °C. It is notable that the samples prepared at 60° and 70 °C did not display endothermic transitions (Fig. 1b). WP may have interfered in the interaction between starch and bixin, competing with the amylose chains by binding to bixin. The increase in protein content led to a decrease in the melting enthalpy ($\Delta H_{melting}$), which had values of 3334.4 J/g for B0WP90°C (0% WP), 1550.4 J/g for B10WP90°C (10% WP) and 1383.8 J/g for B20WP90°C (20% WP). Proteins have a high availability to interact with bixin and this behavior is due, as it was suggested by Zhang and Zhong [22], to an increase in the hydrophobicity of protein in alkaline conditions, which leads to increase the active sites that can binding bixin. The hydrophobicity increases due to higher exposure of tryptophan residues on the surface of protein, after unfolding of the WP chains, as a result of denaturation process and the alkaline pH (close to 11) [30, 31]. The increase in the hydrophobicity of the samples with 10 and 20% of WP was probably a factor that avoided the formation of crystallites with higher size, resulting in a lower energy for their melting, thus leading to a decrease in their melting temperature and $\Delta H_{melting}$. In other starchy systems, the proteins can reduce the binding between amylose and lipids, avoiding the formation of amylose-lipid complexes [20].

X-Ray Diffraction (XRD)

X-ray diffraction patterns of the treated samples and the control are shown in Fig. 2. The samples B0WP90°C, B10WP90°C, B20WP90°C (90 °C) showed slight reflections in the Bragg angles, close to 20°, 14° and 5° (2θ). The samples also displayed a strong diffraction pattern of retrograded amylose, which is suggested by the reflection in the Bragg angle close to 17° and for peaks close to 23° (2θ) similar to those reported by Felker et al. [32] and Czuchajowska et al. [33]. The samples prepared at 60 and 70 °C showed similar diffraction patterns to those prepared at 90 °C. The thermograms do not show endothermic transitions in the temperature range studied, suggesting no formation of crystalline structure type V-amylose.in the treated samples.

The treatments used to prepare the samples resulted in a tendency for decreasing relative crystallinity (Fig. 3) with the increase in WP content. This was probably caused by the interaction between WP and bixin, which can reduce the crystalline order [22]. Samples prepared without WP showed significant differences ($p < 0.05$) in their relative crystallinity. Similarly, the samples at 60 °C and 90 °C, had significant differences in their relative crystallinity compared to the GS-B. These results seem to affect the release of bixin as it will be discussed in the next sections. Both DSC and XRD analyses confirmed the no formation of V-amylose bixin complexes. Nevertheless, at 90 °C a structure possibly formed by WP-Bixin-Starch is formed, which has a crystalline structure with a melting temperature similar to a V-amylose complex type-II.

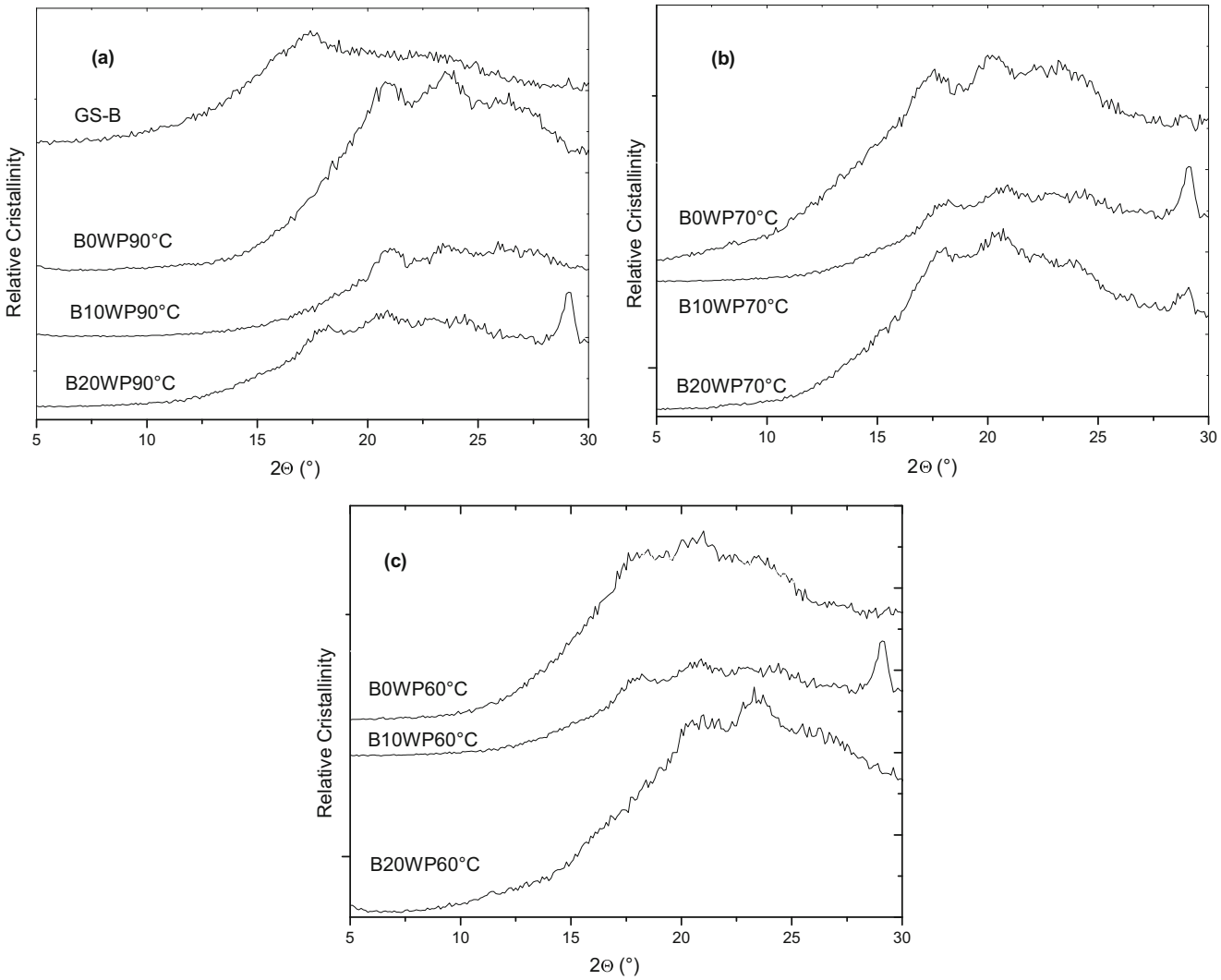

Fig. 2 X-ray diffraction patterns of samples prepared at 90 °C (**a**), 70 °C (**b**) and 60 °C (**c**)

FT-IR Spectroscopy

Figure 4 shows the FT-IR spectra of bixin, GS-WP and GS-B, as well as samples of WP and GS with no treatment. The spectra of bixin showed a band at 1744 cm^{-1} which was associated with stretching vibrations of the –C=O group from aliphatic carboxylic acid, and bands associated with stretching vibrations of conjugated C=C groups at 1613 cm^{-1} (Fig. 4a). Sample GS showed bands between 1200 and 1800 that were correlated with minor components, such as proteins and native lipids present in the starch (Fig. 4b). On the other hand, characteristic bands of proteins called Amide I, II and III display absorption in the regions between 1600 and 1700, 1500–1600 and 1200–1350 cm^{-1}, respectively [34]. In this region, WP displayed bands at 1628 cm^{-1} (Amide I) and 1526 cm^{-1} (Amide II), associated with -C=O and C-N weak stretching and strongly coupled with N-H bending, respectively, as well as a band close to 1231 cm^{-1} (Amide III), which corresponds to twisting of N-H in the plane, coupled with N-N stretching and C-H and N-H deformation vibrations (Fig. 4b). As it is shown in detail (Fig. 4c), the bands at 1310 and 1280 cm^{-1} correspond to α-helix and unordered structure, and the band at 1240 cm^{-1} corresponds to the β-sheet conformation of protein [34]. The low intensity of the band at 1280 cm^{-1} indicates that WP has a lower unordered structure content in comparison to α-helix and β-sheet. GS-WP displayed a combination of bands associated with WP and GS, although the band of Amide III was seen to increase in bandwidth (Fig. 4b). When comparing FT-IR spectra of GS-B, GS-WP and the B0WP90°C, B10WP90°C and B20WP90°C samples, in which an endothermal transition was observed (Fig. 1a), a band at 1744 cm^{-1} associated with the vibration of the –C=O group of bixin was observed. However, a band at 1613 cm^{-1} of conjugated -C=C- groups of bixin disappeared, indicating that vibration of this group was restricted. On the other hand, the FT-IR spectra of B0WP90, B10WP90 and

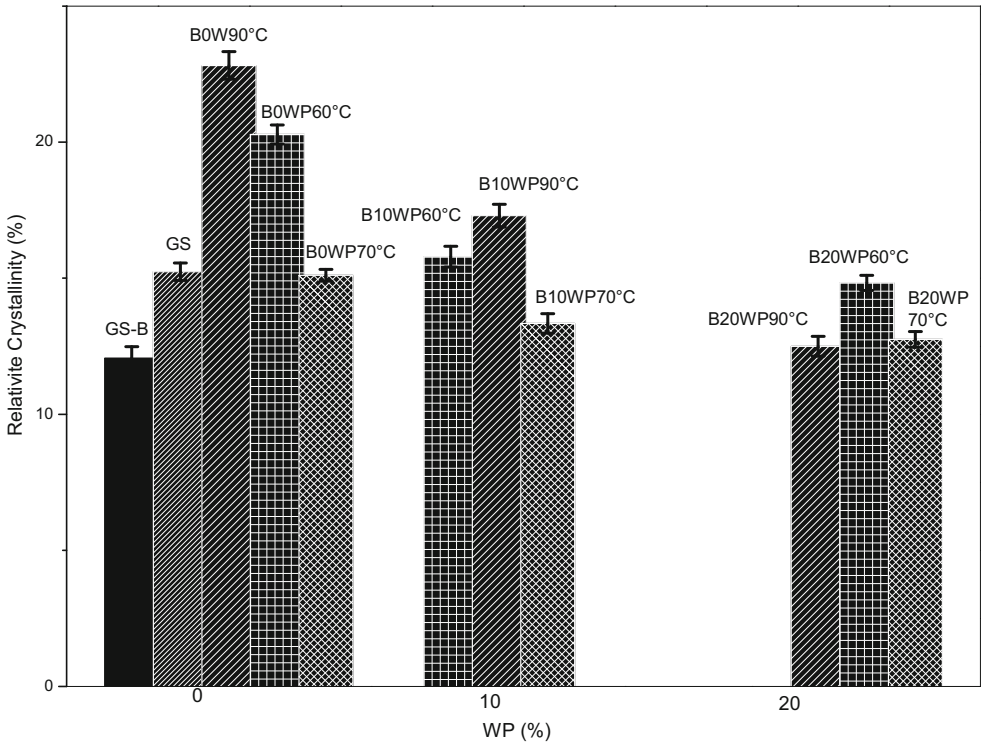

Fig. 3 Relative crystallinity. Samples prepared at 90 °C (b), 70 °C (d) and 60 °C

B20WP90 samples showed narrow bands at the region between 1300 to 1500 cm^{-1} (Fig. 4d) compared to those of GS-WP and GS-B, which were similar to those observed in the GS sample (Fig. 4b). Nevertheless, the spectra of B10WP90°C and B20WP90°C showed a broadband (at the Amide I and Amide II regions) compared to B0WP90 sample. Widening in the bands was associated with the higher WP content. This result indicates that there was an increase in WP availability to interact with bixin. Notwithstanding, these interactions seem to be fewer at a higher temperature of treatment, but enough to affect the thermal stability of the crystalline structures as it was observed in DSC results. On the other hand, after microencapsulation process, the α-helix and β-sheet structures were not observed. This result suggests that the heat treatment and pH affect the secondary structure of WP significantly. The pH can also induce a negative charge on the WP, increasing the repulsion and led to unfolding and loss of the secondary structure of proteins [31]. In other systems such as that formed by casein and bixin, no effects of thermal treatment on casein-bixin binding were observed, due to the higher thermal stability of casein [35]. In contrast, Zhang and Zhong [30] reported that after the thermal process, the hydrophobicity of the β-Lactoglobulin, which is the major component in whey proteins, increases its availability to interact with bixin. In this study, the results suggest that protein and the temperature treatment reduced the interaction between bixin and amylose chains at 60 and 70 °C, probably due to the higher facility of WP to bind to bixin. This is in agreement with Zhang and Zhong [30], who reported that protein-bixin binding is favored at lower temperatures.

Encapsulation Efficiency EE (%)

Figure 6 (Supplementary Figure) shows UV-vis absorption spectra of the bixin and all samples, indicating that there was no hydrolysis or degradation product formation during microencapsulation process. The results of EE are shown in Table 1. The encapsulation efficiency depends on the concentration of starch, protein and its interaction with bixin. The increase in WP content from 10 to 20% lead to decreasing in the EE. The EE decreased from 82.46 to 28.30% at 60 °C, from 57.05 to 34.51% at 70 °C, and from 82.91 to 62.07% at 90 °C (Table 1). This trend was also reported by Rocha et al. [36] and Shu et al. [37] in the encapsulation of lycopene by spray drying using modified starch, and the blend of gelatin and sucrose respectively, both authors reported that higher wall material content induces to lower encapsulation efficiency. The result of bixin encapsulation suggests that 10% of WP correspond to a limit concentration, which is appropriated to reach the higher EE under the three evaluated temperatures (Table 1). The increasing EE observed with WP addition suggested that in the ternary system WP-bixin-starch, the starch seems to act as a matrix-forming material, whereas the protein acts as a film-forming compound that protects the bixin. The film-forming ability of proteins and their capacity of encapsulation is

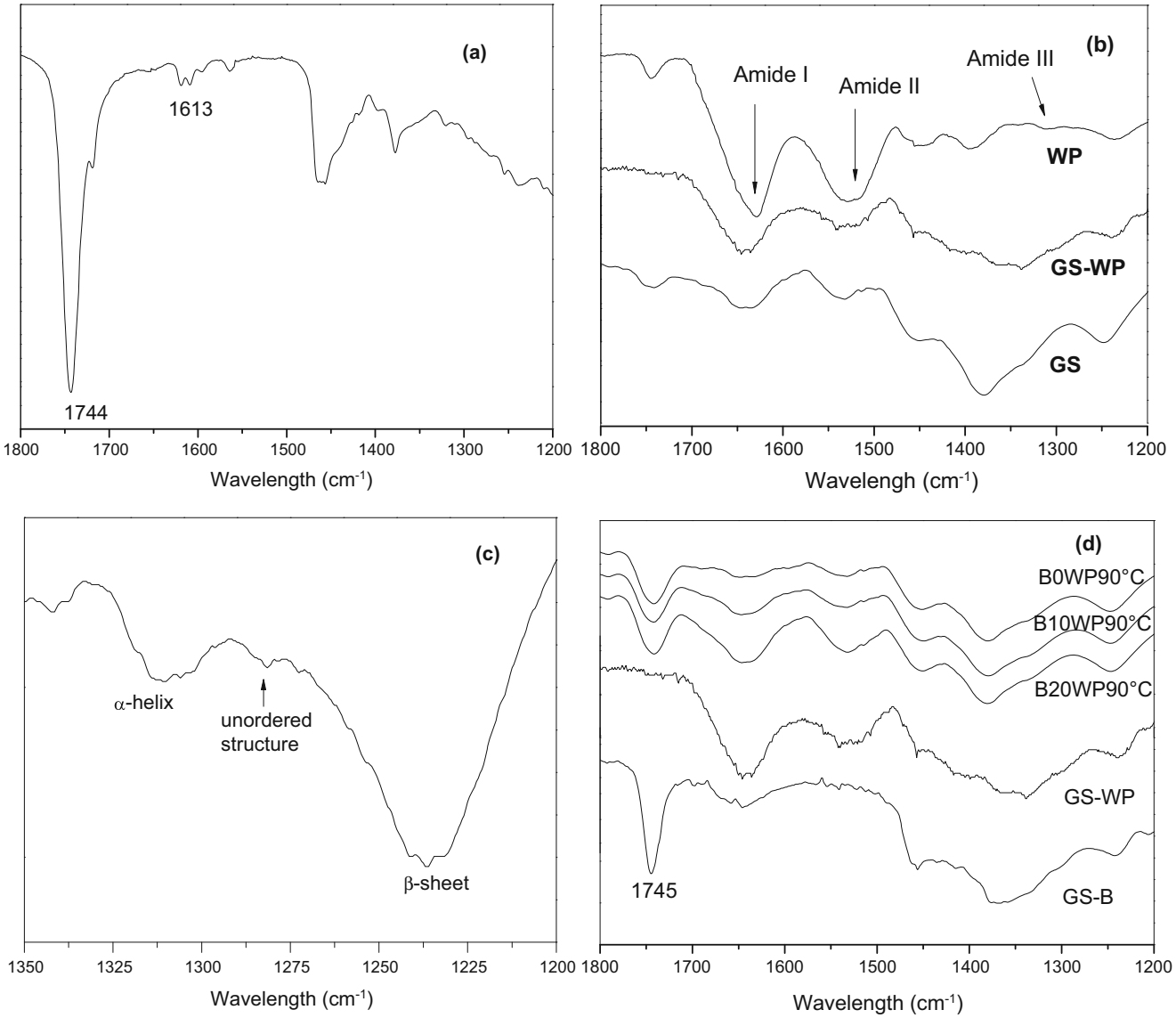

Fig. 4 FT-IR spectra of Bixin (**a**), WP, GS-WP, GS (**b**), α-helix and the β-sheet conformation of WP (**c**), samples at 90 °C (**d**)

known [38]. The EE observed in this study were lower than those reported by De Sousa Lobato et al. [10], which was about 98% in a system prepared by the interfacial deposition of preformed poly-ε-caprolactone. The EE with 10% WP was in the range that has been reported by other researchers using gum Arabic and maltodextrin by spray drying, which ranged between 75 to 86% [9], and higher than that reported by De Marco et al. [39] in the encapsulation of annatto extract by spray drying using a combination of maltodextrin and gum Arabic, which was about 75.7% of efficiency. In addition, the EE in all treatments was in the range reported in the encapsulation of bixin with poly(3-hydroxybutirate-cohydroxyvalerate) and dichloromethane as organic solvent using the technology of supercritical carbon dioxide, which achieved values between 6.36 to 92.02% [40]. In the set of samples prepared at 90 °C was possible to identify crystalline structures by DSC, indicating that, at this temperature level, the interaction bixin-starch was favored in detriment of WP-bixin interaction. On the other hand, it is also known that upon heating, cis-bixin can polymerize to trans-bixin [41, 42], and the trans configuration is less polar than the cis isomer; this transition apparently allows the bixin chains to be partially trapped more easily inside the apolar cavity of amylose

The Release Profile of Bixin

The release profile of samples in simulated intestinal fluid (SIF) is shown in Fig. 5. Samples prepared at 60 °C presented a slightly lower release percent compared to WP-B sample after two hours. Meanwhile, samples prepared at 70 °C with WP had a higher release percent. Samples prepared at 90 °C

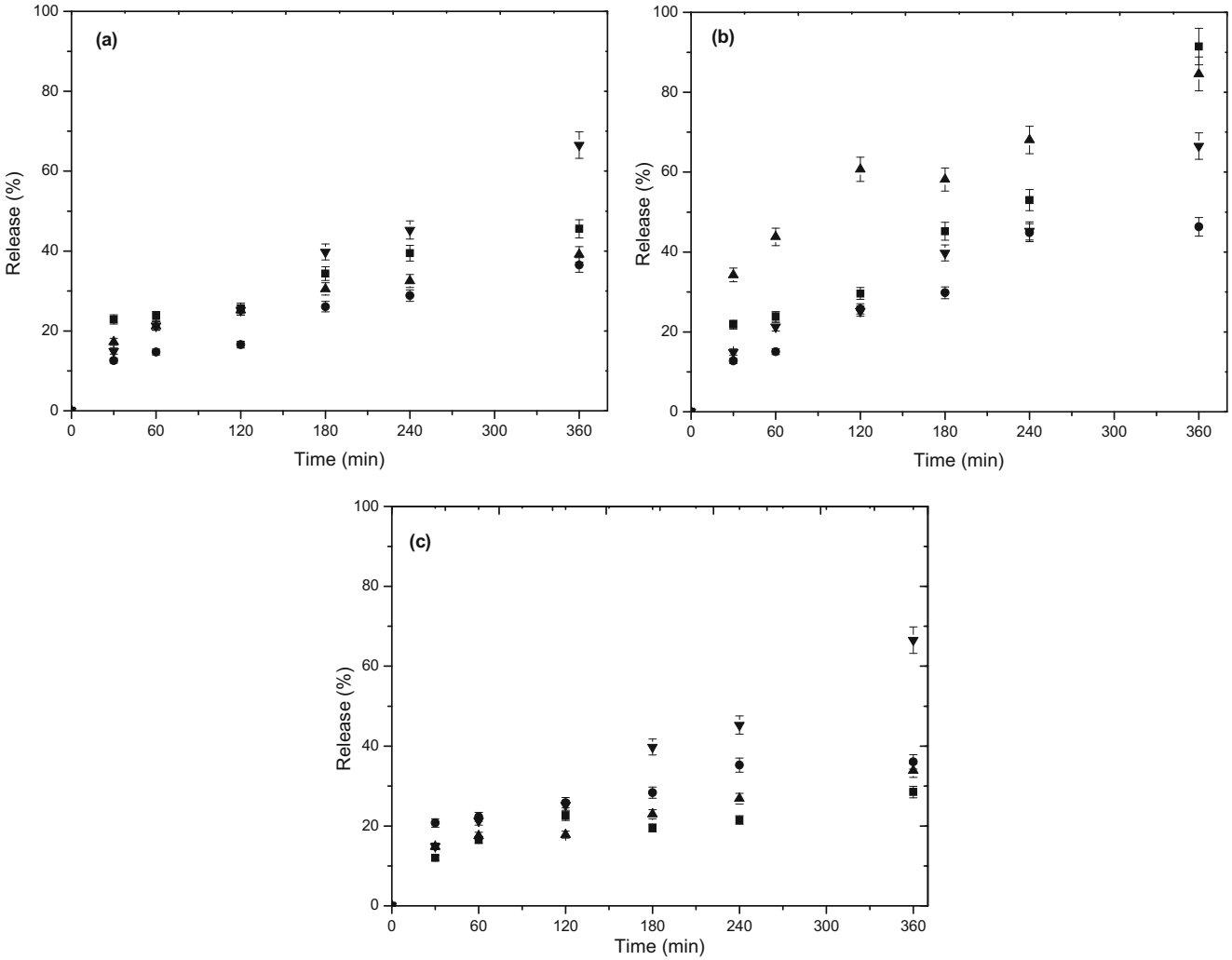

Fig. 5 Bixin-release profiles of samples prepared at 60 °C (**a**), 70 °C (**b**) and 90 °C (**c**). 0% WP (−●-), 10% WP (−■-), 20% WP (−▲-) and GS-B (−▼-)

presented a release percent similar to the control in the first two hours, followed by a stabilization until a nearly constant value was reached, becoming more stable against the action of the SIF. The release pattern is seen to be associated with relative crystallinity percent and treatment temperature. The sample without protein and with a lower crystallinity percent had a trend to shows a higher release percent. Probably, the low crystallinity percent led to a greater effect of the enzymatic action, allowing a higher release percent. This is due to the preference of enzymatic action by amorphous regions [43]. Samples prepared at 60 °C had a release percent of bixin lower than WP-B. Nevertheless, the increase in protein content decreased the release percent. As it was previously discussed, the affinity of the WP for bixin is increased at lower temperature, hindering the SIF action. In samples prepared at 90 °C, an increase in the WP content does not seem to decrease the release percent of bixin. Nevertheless, the release percent of bixin was lower than WP-B. At 70 °C, the WP seems does not have the affinity to binding with bixin. Also, this condition is not appropriate for forming of crystalline structures, resulting in a higher release percent.

Color Analysis

Table 2 (Supplementary Table) shows the color parameters L*, a*, b*, C*, and °hue of the treated and WP-B samples in addition to pure bixin. The parameter L* had higher values in the encapsulated samples than pure bixin, with a trend of being lower than in samples treated at 60 and 70 °C, which can be attributed to the presence of WP and starch. The parameter L* was not affected by the WP content. Regarding parameter a*, in all of the treated samples, a decreasing redness compared to pure bixin was observed. Parameter a* had a tendency to be higher at 70° and 90 °C and lower at 60 °C than the control; this suggests that the redness grows along with the temperature. However, the a* values seem not to rise with the protein content. The treated samples had b* values higher than pure bixin and a pattern of being lower than the control,

indicating a higher yellowness compared to pure bixin. Furthermore, there was a disposition for parameter b* to increase along with a rise in temperature. Concerning chroma C*, the treatment samples presented values in the range between 54.09 and 65.05, which were greater than pure bixin, indicating a higher saturation and consequently a higher intense color. In contrast, parameter C* had values lower than the control, indicating a less intense color, which was probably caused by the thermal treatment. The °hue, which represents the color tonality, varied between 51.73 and 62.3 in the second quadrant of the chromaticity diagram, between red (°hue = 0) and yellow (°hue = 90). In all treatment samples, these parameters had values greater than pure bixin, with the trend of being lower than WP-B. The values of the color parameters suggest that the treatment samples are less red, but with a higher intense color and a tendency to be more red orange than the original color of pure bixin. The color parameters a* and b* of the bixin complex, were higher than those reported by De Sousa Lobato et al. [10], for nanocapsules of bixin (a* = 13.54 and b* = 25.50) in a suspension prepared by interfacial deposition. Moreover, L* had a lower value in comparison to those observed in the treatment samples at 60°, 70° and 90 °C.

Conclusion

The current study carried out the microencapsulation of bixin using high-amylose corn starch and whey protein. Whey protein and microencapsulation process affected the profile and total amount of bixin released under simulated gastrointestinal fluid conditions. The crystalline structure was favored at higher temperature. Amylose is a good wall material, protecting bixin against heat; this was confirmed by the high melting temperature of the crystalline structure. Future studies are desirable to select the best proportions of starch and whey protein, in order to improve the controlled release system.

Acknowledgements The authors thank the Conselho Nacional para o Desenvolvimento Científico e Tecnológico (CNPq, Grant 476927/2012-9) for their financial support.

References

1. R.E. Wrolstad, C.A. Culver, Alternatives to those Artificial FD&C Food Colorants. Annu. Rev. Food Sci. Technol. **3**, 59–77 (2012)
2. P. Giridhar, A. Venugopalan, R.A. Parimalan, Review on annatto dye extraction , analysis and processing – A food technology perspective. JSRR. **3**, 327–348 (2014)
3. C.R. Cardarelli, Benassi M de T, Mercadante AZ. Characterization of different annatto extracts based on antioxidant and colour properties. LWT Food Sci. Technol. **41**, 1689–1693 (2008)
4. M. Abayomi, A.S. Adebayo, D. Bennett, R. Porter, J. Shelly-Campbell, In vitro antioxidant activity of Bixa orellana (annatto) seed extract. JAPS. **4**, 101–106 (2014)
5. A.D.O. Rios, L.M.G. Antunes, L.P. Bianchi M de, Proteção de carotenóides contra radicais livres gerados no tratamento de câncer com cisplatina. Alim. Nutr. **20**, 343–350 (2009)
6. T. Taham, F.A. Cabral, M.A.S. Barrozo, Extraction of bixin from annatto seeds using combined technologies. J. Supercrit. Fluids **100**, 175–183 (2015)
7. K. Balaswamy, P.G. Prabhakara Rao, A. Satyanarayana, D.G. Rao, Stability of bixin in annatto oleoresin and dye powder during storage. LWT Food Sci. Technol. **39**, 952–956 (2006)
8. A.L. Parize, T. Cristina, S.R. De, Maria I, Brighente C, Fávere VT De, et al. microencapsulation of the natural urucum pigment with chitosan by spray drying in different solvents. Afr. J. Biotechnol. **7**, 3107–3114 (2008)
9. M.I.M. Barbosa, C. Borsarelli, A. Mercadante, Light stability of spray-dried bixin encapsulated with different edible polysaccharide preparations. Food Res. Int. **38**, 989–994 (2005)
10. K.B. De Sousa Lobato, K. Paese, J. Casanova, S. Stanisçuaski, A. Jablonski, A. De Oliveira, Characterisation and stability evaluation of bixin nanocapsules. Food Chem. **141**, 3906–3912 (2013)
11. S.M. Lyng, M. Passos, J.D. Fontana, Bixin and α-cyclodextrin inclusion complex and stability tests. Process Biochem. **40**, 865–872 (2005)
12. V.A. Marcolino, G.M. Zanin, L.R. Durrant, M.D.T. Benassi, G. Matioli, Interaction of curcumin and bixin with β-cyclodextrin: Complexation methods, stability, and applications in food. J. Agric. Food Chem. **59**, 3348–3357 (2011)
13. T. Itthisoponkul, J.R. Mitchell, A.J. Taylor, Farhat I a. Inclusion complexes of tapioca starch with flavour compounds. Carbohydr. Polym. **69**, 106–115 (2007)
14. I. Lalush, H. Bar, I. Zakaria, S. Eichler, E. Shimoni, Utilization of amylose-lipid complexes as molecular nanocapsules for conjugated linoleic acid. Biomacromolecules **6**, 121–130 (2005)
15. J.-L. Putaux, M.B. Cardoso, D. Dupeyre, M. Morin, A. Nulac, Hu Y. Single crystals of V-amylose inclusion complexes. Macromol. Symp. **273**, 1–8 (2008)
16. G. Wulff, G. Avgenaki, M.S.P. Guzmann, Molecular encapsulation of flavours as helical inclusion complexes of amylose. J. Cereal Sci. **41**, 239–249 (2005)
17. S. Zabar, U. Lesmes, I. Katz, E. Shimoni, H. Bianco-Peled, Structural characterization of amylose-long chain fatty acid complexes produced via the acidification method. Food Hydrocoll. **24**, 347–357 (2010)
18. C.G. Biliaderis, G. Galloway, Crystallization behavior of amylose-v complexes: Structure-property relationships. Carbohydr. Res. **189**, 31–48 (1989)
19. W.C. Obiro, S. Sinha Ray, M.N. Emmambux, V-amylose structural characteristics, methods of preparation, significance, and potential applications. Food Rev. Intl. **28**, 412–438 (2012)
20. G. Zhang, M.D. Maladen, B.R. Hamaker, Detection of a novel three component complex consisting of starch, protein, and free fatty acids. J. Agric. Food Chem. **51**, 2801–2805 (2003)
21. P. Guerrero, J.P. Kerry, De La Caba K. FTIR characterization of protein-polysaccharide interactions in extruded blends. Carbohydr. Polym. **111**, 598–605 (2014)
22. Y. Zhang, Q. Zhong, Effects of thermal denaturation on binding between Bixin and whey protein. J. Agric. Food Chem. **60**, 7526–7531 (2012)
23. S.C. Sutter, P. Buera, B.E. Elizalde, Beta-carotene encapsulation in a mannitol matrix as affected by divalent cations and phosphate anion. Int. J. Pharm. **332**, 45–54 (2007)

24. D.B. Rodriguez-Amaya, *A Guide to carotenoide analysis in foods* (ILSI PRESS, Washington, D.C, 2001)
25. W. Rahmalia, J.-F. Fabre, T. Usman, Z. Mouloungui, Aprotic solvents effect on the UV-visible absortion spectra of bixin. Spectrochim. Acta A Mol. Biomol. Spectrosc. **131**, 455–460 (2014)
26. D. Tupuna, K. Paese, S. Guterres, A. Jablonski, S. Flôres, A. Rios, Encapsulation e fficiency and thermal stability of norbixin microencapsulated by spray-drying using different combinations of wall materials. Ind. Crop Prod. **111**, 846–855 (2018)
27. U. Lesmes, J. Barchechath, E. Shimoni, Continuous dual feed homogenization for the production of starch inclusion complexes for controlled release of nutrients. Innovative Food Sci. Emerg. Technol. **9**, 507–515 (2008)
28. J. Kim, T. Seo, S. Lim, Preparation of aqueous dispersion of b-carotene nano-composites through complex formation with starch dextrin. Food Hydrocoll. **33**, 256–263 (2013)
29. J. Karkalas, S. Ma, W.R. Morrison, Pethrick R a. Some factors determining the thermal properties of amylose inclusion complexes with fatty acids. Carbohydr. Res. **268**, 233–247 (1995)
30. Y. Zhang, Q. Zhong, Binding between bixin and whey protein at pH 7.4 studied by spectroscopy and isothermal titration calorimetry. J. Agric. Food Chem. **60**, 1880–1886 (2012)
31. F.J. Monahan, J.B. German, J.E. Kinsellat, Effect of pH and temperature on protein unfolding and thiol/ disulfide interchange reactions during heat-induced gelation of whey proteins. J. Agric. Food Chem. **43**, 46–52 (1995)
32. F.C. Felker, J.A. Kenar, G.F. Fanta, A. Biswas, Comparison of microwave processing and excess steam jet cooking for spherulite production from amylose-fatty acid inclusion complexes. Starch-Starke **65**, 864–874 (2013)
33. Z. Czuchajowska, D. Sievert, Y. Pomeranz, Enzyme-resistant starch . IV . Effects of Complexing Lipids. Cereal Chem. **68**, 537–542 (1991)
34. B.R. Singh, in *Infrared Analysis of Peptides and Proteins: Principles and Aplication*, ed. by B. R. Sing. Basic aspects of the technique and applications of infrared spectroscopy of peptides and proteins (ACS symposium serie, Washington, D.C, 2000), p. 190
35. Y. Zhang, Q. Zhong, Encapsulation of bixin in sodium caseinate to deliver the colorant in transparent dispersions. Food Hydrocoll. **33**, 1–9 (2013)
36. G.A. Rocha, C.S. Fávaro-Trindade, C.R.F. Grosso, Microencapsulation of lycopene by spray drying: Characterization, stability and application of microcapsules. Food Bioprod. Process. **90**, 37–42 (2012)
37. B. Shu, W. Yu, Y. Zhao, X. Liu, Study on microencapsulation of lycopene by spray-drying. J. Food Eng. **76**, 664–669 (2006)
38. A. Madene, M. Jacquot, Review flavour encapsulation and controlled release – A review. Int. J. Food Sci. Technol. **41**, 1–21 (2006)
39. R. De Marco, A.M.S. Vieira, M.C.A. Ugri, A.R.G. Monteiro, R.D.C. Bergamasco, Microencapsulation of annatto seed extract: Stability and application. Chem. Eng. Trans. **32**, 1777–1782 (2013)
40. D.L. Boschetto, R.A. Loss, G.N. Pereira, G.S.P. Aguiar, J.R. Machado, L.M.P.C. Chaves, et al., Encapsulation of eugenyl acetate in PHBV using SEDS technique and in vitro release evaluation. J. Food Sci. Technol. **53**, 3859–3864 (2014)
41. M.A. Montenegro, A.D.O. Rios, A.Z. Mercadante, M.A. Nazareno, C.D. Borsarelli, Model studies on the photosensitized isomerization of Bixin. J. Agric. Food Chem. **52**, 367–373 (2004)
42. O. Rios A de, C. Borsarelli, M. Adriana, Thermal degradation kinetics of Bixin in an aqueous model system. J. Agric. Food Chem. **53**, 2307–2311 (2005)
43. J.a. Putseys, L. Lamberts, J.a. Delcour, Amylose-inclusion complexes: Formation, identity and physico-chemical properties. J. Cereal Sci. **51**, 238–247 (2010)